POROUS MEDIA APPROACH IN THERMAL-HYDRAULIC CORE ANNALYSIS OF PRESSURIZED WATER REACTORS

*G. JAHANFARNIA, M.H. RAHIMI**

Department of Engineering, Science and Research Branch, Islamic Azad University, Tehran, Iran

rezajahan@yahoo.com
m.h.rahimi@gmx.com

ABSTRACT

Researches and studies on nuclear reactor core are usually subdivided into two major fields, named: Thermal-Hydraulic and Neutronic, in which, precise simulation of reactor behaviour in both fields is highly required to ensure the designers that reactor will work in a safe margin. In this study, a thermal-hydraulic analysis of pressurized water reactor core is performed using a porous media approach. Based on this approach, each fuel assembly was modelled and was divided into a network of lumped regions; each of them was characterized by a volume average parameter. In such manner, while complex geometries are easily defined and dealt with, the thermal-hydraulic parameter and phenomena like friction, shear stress, cross-flows, convective heat transfer and etc. are strictly included in simulations. To validate the applied approach, the numerical analysis and COBRA EN code results were compared for a typical PWR core and showed a good agreement.

Key words: Thermal-hydraulic, Core analysis, Porous media

Introduction

The early design of nuclear reactors prototype was introduced in 1950's and commissioning of the first industrial nuclear power plants was started in 1960's. A huge effort was dedicated since then on studies and researches about nuclear related phenomena and simulation methods. Today, after six decades we can almost say all nuclear related phenomena in industrial scale, are well known and further efforts are targeted to aim an optimized calculation method in order to achieve a fast and precise simulation of reactor core behaviour.

A serious issue in the thermal-hydraulic modelling of a reactor core is that the core itself is a complex structure and the presence of fluid, which gives rise to complex damping, added mass effects, turbulence effects and fuel assembly coupling processes [4].To deal whit such a complex problem, there are two commonly used methods for simplifying and analysing the thermal-hydraulic behaviour of the coolant flow in the reactor core, named: the porous media approach and the sub-channel approach [3]. From engineering point of view, the sub-channel approach is a simplified version of the porous media one, with an inherent assumption of the existence of a dominantly axial flow in system [2]. While this method is used in a variety number of core calculation studies [5-9], but it is doubtful that the sub-channel method

can be applied in strong cross flow cases such as a flow blockage or a degraded core geometry, which is encountered in a liquid metal fast birder reactor (LMFBR) safety analysis [2].

G. Ricciardi applied the porous media approach for analysing the thermal-hydraulic behaviour of a pressurized water reactor [4] and E. Zarifi used this method for the steady state analysis of a reactor core [8]. This approach was developed to provide an alternative for the rod bundle analysis and for application to the general flow cases. The porous body approach is formulated based on the porosities of the control volume for which the conservation equations are written. This allows an arbitrary geometric configuration for the control volume because the geometric effect is taken into account through the surface and volume porosities. In addition, this approach solves the transverse momentum equation as well as the axial momentum equation rigorously. This study proposed the transient-state analysis of a typical Pressurized Water Reactor using the porous media method.

Material and methods

Consider a domain consisting of a single-phase fluid and distributed solids. Initially, the solids will be assumed as deformable but stationary in space so that the resulting equations may also be applied to describe a two-phase situation. Heat may be generated or absorbed by the solid structure. For an arbitrary point in the domain, we associate a closed surface A_T as enclosing a volume, V_T. The portion of V_T which contains the fluid is V_f The total fluid-solid interface within the volume V_T is A_{fs}. The portion of A_T through which the fluid may flow is A_f. A schematic of the control volume is illustrated in **Figure 1**.

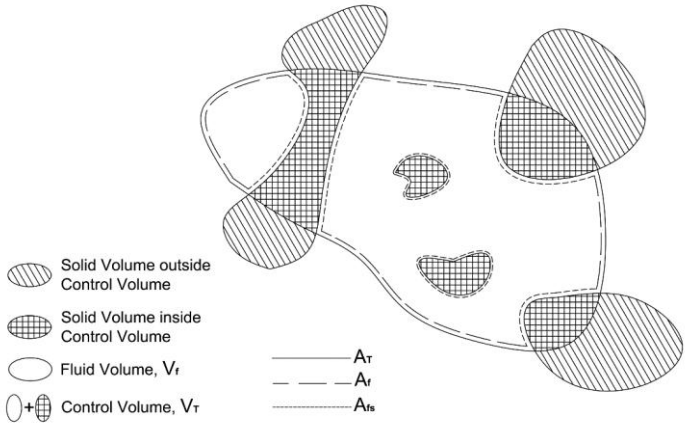

Figure 1 *Region consisting of a single-phase fluid with stationary solids.*

The ratio of fluid volume V_f to the total volume V_T is defined as the volume porosity γ_v .Thus:

$$\gamma_V = \frac{V_f}{V_T}, \tag{1}$$

And the mathematical definition of the surface porosity γ_A associated with any surface (not necessarily closed) is:

$$\gamma_A = \frac{A_f}{A_T}, \tag{2}$$

Where A_f is the portion of A_T which is occupied by the fluid. The notations used in the following relations are summarized in **Figure 2**.

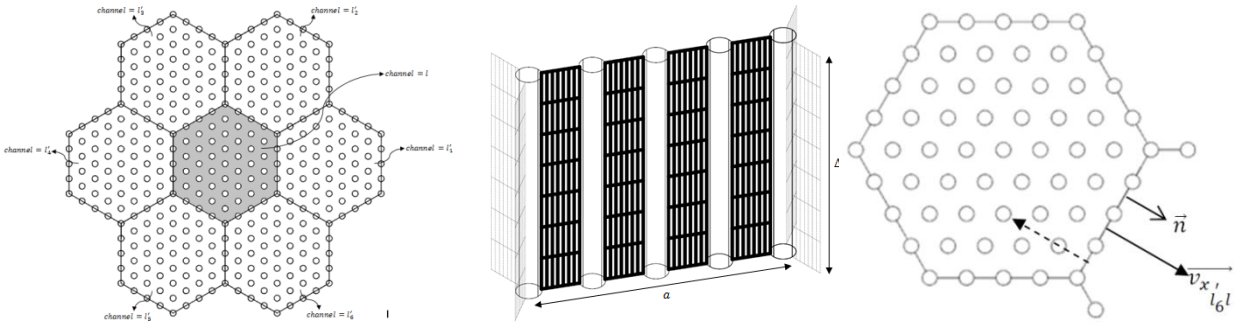

A B C

Figure 2 A) *Cross section of 7 hypothetical fuel assemblies, connected transversely to each other. B) The cross flow surface between channel l'_6 and l. C) The normal vector of cross flow surface and velocity between channel l'_6 and l.*

The differential forms of the mass, linear momentum and energy (in terms of enthalpy) conservation equations [3] after performing the volume and surface averaging as the well as porosity definition yield respectively as follows:

$$\gamma_V \frac{\partial^i \langle \rho \rangle}{\partial t} + \frac{1}{V_T} \int_{A_f} \rho \vec{v}.\vec{n} dA = 0, \tag{3}$$

$$\gamma_V \frac{\partial^i \langle \rho \vec{v} \rangle}{\partial t} + \frac{1}{V_T} \int_{A_f} \rho \vec{v}(\vec{v}.\vec{n}) dA = \gamma_V {}^i\langle \rho \rangle \vec{g} + \frac{1}{V_T} \int_{A_f} (-P.\vec{n} + \bar{\bar{\tau}}.\vec{n}) dA + \gamma_V {}^i\langle \vec{R} \rangle, \tag{4}$$

$$\gamma_V \frac{\partial}{\partial t}{}^i\langle \rho U \rangle + \frac{1}{V_T} \int_{A_f} \rho U \vec{v}.\vec{n} dA = -\gamma_V {}^i\langle P \nabla.\vec{v} \rangle + \gamma_V \left(\langle q'''_{rb} \rangle + {}^i\langle q''' \rangle \right) \tag{5}$$

The mathematical symbols $\langle\ \rangle$, ${}^i\langle\ \rangle$ and $\bar{\bar{\tau}}$ designate that the average is associated with the whole volume, the fluid flow volume of the control-volume and the surface, respectively. The distributed resistance $\vec{R}$ is a key concept associated with the porous media approach and is the resistance force per unit volume of fluid that is exerted on the fluid by the dispersed solid. An equivalent but oppositely directed force is exerted on the dispersed solid by the fluid and is an effective drag force per unit volume of fluid. For example, for axial flow, by recognizing that there is no form drag and by applying a force balance, one can easily obtain:

$${}^i\langle R_z \rangle = \frac{1}{V_f} \vec{k}. \int_{A_{fs}} \bar{\bar{\tau}}.\vec{n} dA = -\frac{\Delta P_{friction} A_f}{V_f} = -\frac{\Delta P_{friction}}{\Delta z} = f \frac{\Delta z}{D_e} \frac{{}^i\langle \rho \rangle {}^i\langle v_z \rangle^2}{2}\ , \tag{6}$$

The manipulation of Eq. (3) and (4) will proceed to the following results, respectively:

$$\frac{\partial^{i}\langle\rho\rangle}{\partial t}+\frac{\partial\left(\rho v_{z}\right)}{\partial z}=\frac{1}{\gamma_{V}V_{T}}\sum_{i=1}^{6}s_{l_{i}^{'}l}\left(\rho v_{x_{l_{i}^{'}l}}\right) \tag{7}$$

$$\begin{aligned}\frac{\partial}{\partial t}^{i}\langle\rho v_{z}\rangle+\frac{\partial\left(\rho v_{z}^{2}\right)}{\partial z}&=-^{i}\langle\rho\rangle g_{z}+^{i}\left\langle\vec{R}\right\rangle-\frac{\partial\left(P\right)}{\partial z}+\frac{\partial\left(2\mu\frac{\partial\left(v_{z}\right)}{\partial z}+\frac{2}{3}\mu(\nabla.\vec{v})\right)}{\partial z}\\&-\frac{1}{\gamma_{V}A_{Tz}}\sum_{i=1}^{6}\left(s_{l_{i}^{'}l}\frac{\partial}{\partial x_{l_{i}^{'}l}}\left[\mu\left(\frac{\partial\left(v_{z}\right)}{\partial x_{l_{i}^{'}l}}+\frac{\partial\left(v_{l_{i}^{'}l}\right)}{\partial z}\right)\right]\right)+\frac{1}{\gamma_{V}A_{Tz}}\sum_{i=1}^{6}s_{l_{i}^{'}l}\left(\rho v_{z}v_{x_{l_{i}^{'}l}}\right)\end{aligned} \tag{8}$$

Or Shortly:

$$\frac{\partial}{\partial t}^{i}\langle\rho v_{z}\rangle+\frac{\partial\left(\rho v_{z}^{2}\right)}{\partial z}=-^{i}\langle\rho\rangle g_{z}+^{i}\left\langle\vec{R}\right\rangle-\frac{\partial\left(P\right)}{\partial z}+\Lambda+\frac{1}{\gamma_{V}A_{Tz}}\sum_{i=1}^{6}s_{l_{i}^{'}l}\left(\rho v_{z}v_{x_{l_{i}^{'}l}}\right) \tag{9}$$

Where, g_{z} is the gravity acceleration along the axial direction. Λ and $s_{l_{i}^{'}l}$ are:

$$\Lambda=\frac{\partial\left(2\mu\frac{\partial\left(v_{z}\right)}{\partial z}+\frac{2}{3}\mu(\nabla.\vec{v})\right)}{\partial z}+\frac{1}{\gamma_{V}A_{Tz}}\sum_{i=1}^{6}\left(s_{l_{i}^{'}l}\frac{\partial}{\partial x_{l_{i}^{'}l}}\left[\mu\left(\frac{\partial\left(v_{z}\right)}{\partial x_{l_{i}^{'}l}}+\frac{\partial\left(v_{l_{i}^{'}l}\right)}{\partial z}\right)\right]\right). \tag{10}$$

$$s_{l_{i}^{'}l}=\frac{A_{f_{l_{i}^{'}l}}}{\Delta z}, \tag{11}$$

Defining a state relation as:

$$\frac{\partial\rho}{\partial t}=\frac{\partial\rho}{\partial P}\frac{\partial P}{\partial t}+\frac{\partial\rho}{\partial T}\frac{\partial T}{\partial t}=G1\frac{\partial P}{\partial t}+G2\frac{\partial T}{\partial t}, \tag{12}$$

And applying it to the conservation of mass and energy equations (Eq. (7) and Eq. (5), respectively) will result in:

$$G1\frac{\partial P}{\partial t}+G2\frac{\partial T}{\partial t}+\frac{\partial\rho v_{z}}{\partial z}=\frac{1}{\gamma_{V}V_{T}}\sum_{i=1}^{6}s_{l_{i}^{'}l}\rho v_{x_{l_{i}^{'}l}}, \tag{13}$$

$$(\rho c_{V}+U.G2)\frac{\partial T}{\partial t}+U.G1\frac{\partial P}{\partial t}+\frac{\partial\rho Uv_{z}}{\partial z}=\frac{1}{\gamma_{V}A_{Tz}}\sum_{i=1}^{6}s_{l_{i}^{'}l}\rho Uv_{x_{l_{i}^{'}l}}+q_{rb}^{'''}+q^{'''}-P\frac{\partial v_{z}}{\partial z}, \tag{14}$$

By merging these two last equations together and rewriting it in the form of a matrix, we obtain the desired relation:

$$\begin{bmatrix}G1 & G2\\ U.G1 & \rho c_{V}+U.G2\end{bmatrix}\frac{\partial\begin{bmatrix}P\\ T\end{bmatrix}}{\partial t}+\frac{\partial\begin{bmatrix}\rho v_{z}\\ \rho Uv_{z}\end{bmatrix}}{\partial t}=\begin{bmatrix}\frac{1}{\gamma_{V}V_{T}}\sum_{i=1}^{6}s_{l_{i}^{'}l}\rho v_{x_{l_{i}^{'}l}}\\ \frac{1}{\gamma_{V}A_{Tz}}\sum_{i=1}^{6}s_{l_{i}^{'}l}\rho Uv_{x_{l_{i}^{'}l}}+q_{rb}^{'''}+q^{'''}-P\frac{\partial v_{z}}{\partial z}\end{bmatrix}, \tag{15}$$

Or shortly:

$$G\frac{\partial Q}{\partial t}+\frac{\partial v_z F}{\partial t}=S. \tag{16}$$

To obtain the axial velocity, we can easily apply Eq. (7) into Eq. (9). The final result can be written as:

$$\rho\frac{\partial v_z}{\partial t}+\frac{\rho}{2}\frac{\partial v_z^2}{\partial t}=-\frac{\partial P_z}{\partial z}-\rho g_z+R_z-\Lambda. \tag{17}$$

Two mechanisms create the transverse mass flows: the transverse pressure gradients that drive diversion cross-flow and the turbulent fluctuations in the axial flow that drive the turbulent mass interchanges.

In a reactor core, the transverse pressure gradients can be established by one of two types of phenomena: geometry variations or non-uniform changes in the fluid density. Geometry variations include fuel rod bowing and swelling, whereas density changes encompass the small differences across a bundle due to the radial heat flux variations and the large local difference due to the onset of boiling**.** The magnitude of diversion cross-flow rate is small compared with the axial flow under the reactor operational conditions except in cases such as flow blockage or fuel rod bowing**.**

This exchange is postulated to involve equal volumes of eddies which cross a transverse sub-channel boundary. If these eddies are also of equal density as they effectively are for single-phase flow conditions, then no net mass exchange results. However, in two-phase flow, a net mass exchange can occur. In single-phase flow although no net mass exchange occurs, both momentum and energy are exchanged between the sub-channels, and their rates of exchange are characterized in terms of hypothetical turbulent interchange flow rates.

Cross-Flow relations are described in reference. No 3. These relations are included in the developed code with the following equation:

$$w_{l_i^{'}l}=s_{l_i^{'}l}\,\rho v_{x_{l_i^{'}l}} \tag{18}$$

As seen in the program flow-chart (**Figure 3**), in each time-loop, the coolant pressure of each channel is obtained individually. Then by using calculated pressures, the axial velocity along each fuel assembly is computed. Finally, the coolant temperature will be calculated. Other properties of the coolant are obtained by using the pressure, velocity, temperature and the thermo dynamic table of water [1].

Applying a proper calculation method will lead to the attainment of convergence of the steady state with a rapid convergence of the results.

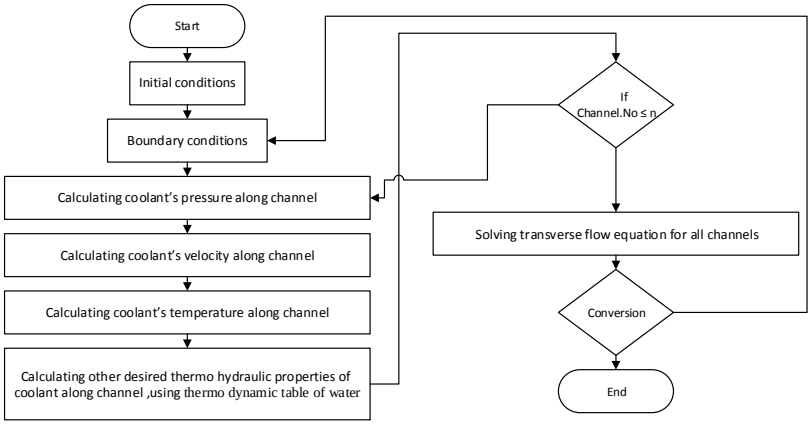

Figure 3 *Calculation flow chart*

Results and discussion

In order to validate the proposed model, we simulated a Typical PWR core based on porous media approach and we compared the results with COBRA-EN code outputs. Basic characteristics of the considered reactor are listed in **Table 1**. Calculations are performed in each fuel assembly for 15 axial mesh points with boundary conditions of: a) Average coolant velocity at the core inlet= 5.6 *m/s* b) Coolant temperature at the reactor inlet= 291 ^{o}C and c) Coolant pressure at the reactor outlet= 15.9 *MPa*. The initial conditions are taken as equal to those of the boundary conditions in these calculations. The time step is 0.0001 s using $\Delta t \leq \Delta z/(c+v_{ave})$ where Δt, Δz, c and v_{ave} are the time step, axial step, the sound speed in the coolant and the average velocity of the coolant, respectively [3].

Table 1 *Main parameters of a typical PWR [9]*

Parameter	Value
Reactor nominal thermal power, *MW*	3000
Coolant pressure at the core outlet, *MPa*	15.9
Coolant temperature at the reactor inlet, °*C*	291
Coolant temperature at the reactor outlet, °*C*	321
Average coolant velocity at the core inlet, *m/s*	5.6
Number of loops	4
Fuel height in the core in cold state, *m*	3.53
Equivalent diameter of the core, *m*	3.16
Number of fuel assemblies in the core	163
Pitch between FAs, *m*	0.236
Number of fuel rods in a fuel assembly	311
Pitch between the fuel rods, *m*	0.01275
Number of Spacing grid along a fuel assembly	15

Pressure calculation in compressible fluids is quite critical parameter. While propagation of pressure wave in fluid is a function of sound speed, any changes in pressure will be sensed all over reactor core in a short period of time. In **Figure 4**, the calculated average pressure for the coolant at half-height of the reactor core starts to fluctuate a user defined initial value as an initial condition. As one can see, this parameter gets to its steady state in a short period of time (0.3 s).

As we mentioned in **Figure 4**, after pressure is calculated, velocity of coolant will be obtained from this pressure in each time step. Therefore, we expect the same fluctuation for the velocity as well. See **Figure 5**.

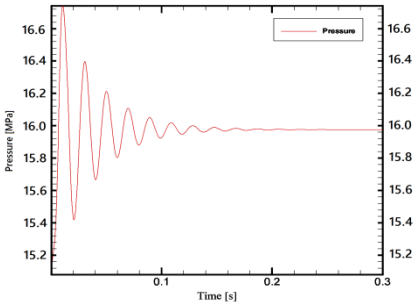

Figure 4 *Average coolant's pressure of a typical PWR at the middle of its core.*

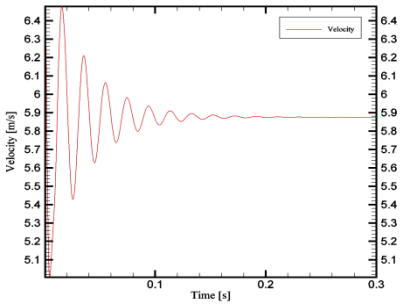

Figure 5 *Average coolant's velocity of a typical PWR at the middle of its core.*

Contrary to pressure and velocity, fluctuation of enthalpy and density are transmitted though the coolant by a diffusion phenomenon which is a delayed function. **Figure 6** and **Figure 7** show the variation of the average coolant enthalpy and density, respectively. As one can see, the enthalpy and density reach their steady state at t=0.6*s*, while the pressure reaches its steady state at t=0.3 s.

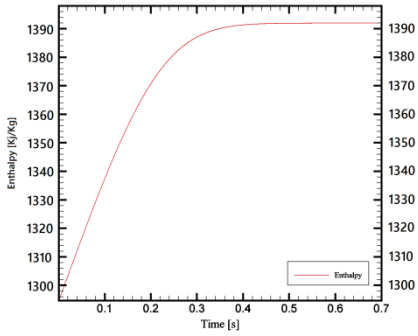

Figure 6 *Average coolant's enthalpy of a typical PWR at the middle of its core.*

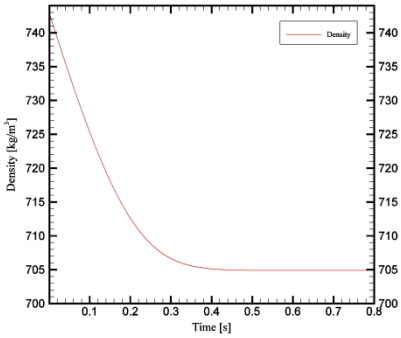

Figure 7 *Average coolant's density of a typical PWR at the middle of its core.*

The pressure drop in the fuel-assemblies includes: a) continuous and linear pressure drop due to coolant-wall friction b) Abrupt pressure drops due to geometry changes through a channel, especially on grid spacers. **Figure 8** shows the effect of these two phenomena on the average coolant pressure of a typical PWR over its axial core length.

Thermal energy generated in the fuel is transferred to the coolant flowing through the fuel assembly. In cylindrical cores, the axial heat-generation distribution has a cosine form of $q=q_{max}Cos(nz/L)$, where q, z and L are the volumetric heat-generation, the axial length and the active fuel rod length, respectively. The rate of heat transfer to the coolant and the enthalpy/temperature rise in the fluid reach their maximums at the axial half-length of the fuel rods. See **Figure 9** and **Figure 10**. Density is a rivers function of enthalpy and is calculated with state relations proposed in IAPWS-IF97 [1]. See **Figure 11**.

Comparing the output results between the developed program and the COBRA-EN code in **Figure 9**, **Figure 10** and **Figure 11** show a good agreement, which in turn emphasizes the accuracy of the final results (Max error < 1.5%).

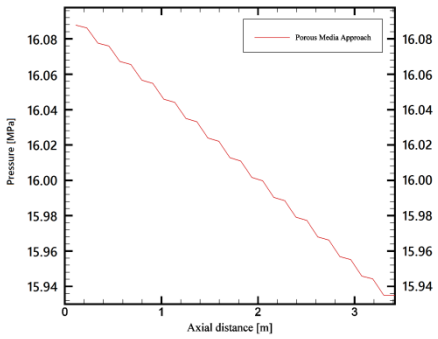

Figure 8 *Average coolant pressure of a typical PWR over its axial core length.*

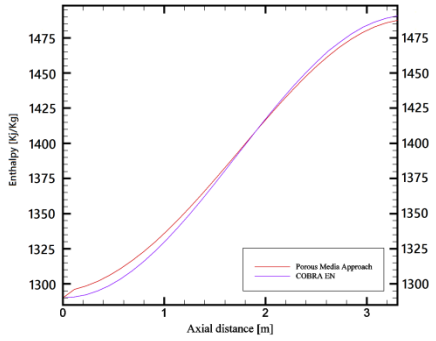

Figure 9 *Average coolant enthalpy of a typical PWR over its axial core length.*

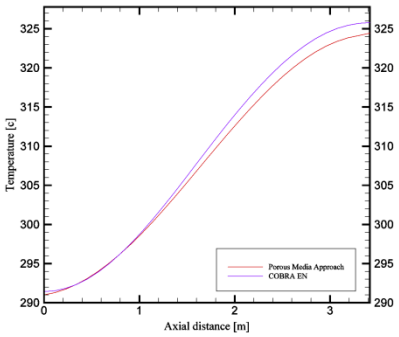

Figure 10 *Average coolant temperature of a typical PWR over its axial core length.*

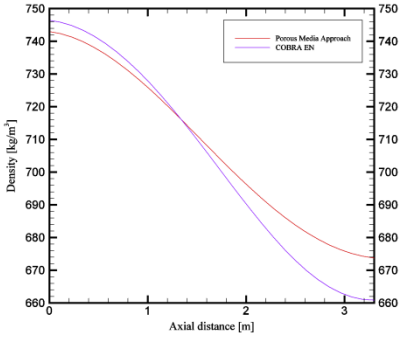

Figure 11 *Average coolant density of a typical PWR over its axial core length.*

According to the continuity equation and the reduction of density along the reactor core, the coolant velocity would subsequently increase. See **Figure 12**.

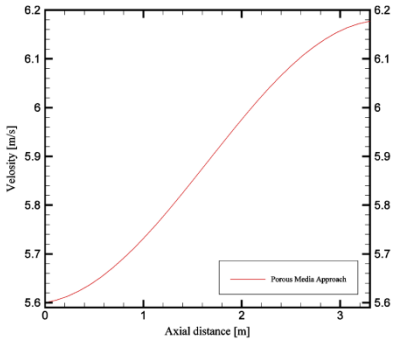

Figure 12 *Average coolant velocity of a typical PWR over its axial core length.*

Conclusion

In the present paper, the pressure, velocity and temperature distributions of the coolant in a PWR are evaluated using the porous media approach. The required thermodynamic properties of the coolant such as enthalpy and density are carried out using IAPWS IF97. This simulation shows that:

- The axial pressure drop of the coolant that flows through the fuel-assemblies is due to the coolant-wall friction and the abrupt geometry changes through a channel, especially on grid spacers.
- The temperature (or enthalpy) increment rate in the middle third of the fuel assemblies reaches its maximum due to the cosine shape of the heat generation through the fuel-assembly height. Consequently, the maximum reduction rate of the density would be obtained in this position.
- According to the continuity equation and the reduction of the density along the reactor core, as water flows from lower plenum to the upper one, the coolant velocity would subsequently increase.

Comparing the output results between the developed program and the COBRA-EN code, a good agreement can be seen, which in turns emphasizes the precision of the porous media approach for the reactor core enthalpy and the accuracy of the final results.

References

[1] W. Wagner, H.J. Kretzschmar, International Steam Tables, Properties of Water and Steam Based on the Industrial Formulation IAPWS-IF97, Second edition, Springer, 2008.

[2] T.S. Ro, Trans. Porous Body Analysis of Vertical Rod Bundles Under Mixed Convection Condition, PhD thesis, Department of Nuclear Engineering, Massachusetts Institute of Technology, 1986

[3] N.E. Todreas, M.S. Kazimi, Nuclear Systems II Elements of Thermal Hydraulic Design, Taylor & Francis, 2001.

[4] G. Ricciardi, S. Bellizzi, B. Collard, B. Cochelin, Modeling Pressurized Water Reactor cores in terms of porous media, Journal of Fluids and Structures.25, 2008, p. 112–133

[5] W.K. In, D.H. Hwang, J.J. Jeong, A subchannel and CFD analysis of void distribution for the BWR fuel bundle test benchmark, Nuclear Engineering and Design, 258, 2013,p. 211–225

[6] J. Weisman, S.H. Ying, A theoretically based critical heat flux prediction for rod bundles at PWR conditions, Nuclear Engineering and Design, 85, 1985, p. 239–250

[7] E. Zarifia, G. Jahanfarniaa, F. Veysi, Subchannel analysis of nanofluids application to VVER-1000 reactor, Chemical Engineering Research and Design, 91, 2013, p. 625-632

[8] E. Zarifia, G. Jahanfarniaa, F. Veysi, Thermal–hydraulic modeling of nanofluids as the coolant in VVER-1000 reactor core by the porous media approach, Annals of Nuclear Energy, 51, 2013, p. 203–212

[9] M. Memmott, J. Buongiorno, P. Hejzlar, On the use of RELAP5-3D as a subchannel analysis code, Nuclear Engineering and Design, 240, 2010, p. 807–815